Analytical Biochemistry 393 (2009) 149–154

Contents lists available at ScienceDirect

Analytical Biochemistry

journal homepage: www.elsevier.com/locate/yabio

Surface-enhanced Raman spectroscopy combined with atomic force microscopy for ultrasensitive detection of thrombin

Anna Rita Bizzarri *, Salvatore Cannistraro

Biophysics and Nanoscience Centre, CNISM, Facolta' di Scienze, Università della Tuscia, I-01100 Viterbo, Italy

ARTICLE INFO

Article history:
Received 7 January 2009
Available online 27 June 2009

Keywords:
Thrombin
Surface-enhanced Raman spectroscopy (SERS)
Atomic force microscopy (AFM)
Gold nanoparticles

ABSTRACT

We have developed an ultrasensitive analytical method based on surface-enhanced Raman spectroscopy (SERS) exploiting a Raman probe covalently bound to gold nanoparticles. The biological marker to be detected was adsorbed on functionalized gold nanoparticles. The capture of these nanoparticles via a biorecognition process between the marker and the immobilized receptor was demonstrated by atomic force microscopy (AFM) imaging. The vibrational fingerprints of the Raman probe on the capture substrate were followed to reveal the presence of the biological marker. The method, which was applied to reveal thrombin captured on a substrate containing antithrombin and heparin, resulted in the ability to detect marker concentrations down to the picomolar (pM) level.

Specific recognition between two biological partners is widely exploited in biosensors nowadays such as for detection of environmental pollutants, in early and clinical diagnostics, and for screening of pharmaceutical chemicals [1,2]. Once the complex between the two partners is formed, different readout tools can be used for detection; examples of commonly applied techniques include fluorescence, surface-enhanced Raman spectroscopy (SERS)[1], surface plasmon resonance, electrochemistry, and quartz crystal microbalance [3–5].

SERS, which can reach single molecule detection with a rewarding chemical specificity [6–9], offers high potentialities in early biodiagnostics if coupled with biorecognition events, as witnessed by recent pioneering research [10–14]. SERS is based on the huge enhancement of the Raman cross section of molecules when they are placed in the proximity of a nanostructured metal surface as due to the contribution of an electromagnetic (EM) and chemical effect [15–18]. In general, SERS spectra arise from a superposition of signals from a few molecules at active "hot spots" characterized by a highly enhanced Raman cross section, with the preponderant molecules at the other sites ("cold sites") giving a much lower contribution to the final spectrum [19]. Moreover, the SERS phenomenon is regulated by several factors that are difficult to control and reproduce such as the roughness of the metal surface, the distance and orientation of the Raman probe with respect to the surface, and the electronic coupling between the molecule and the metal [15]. In particular, the distance of the probe to the metal surface has been found to play a dominant role in determining the final enhancement [20] that, on the other hand, can be maximized when coupled with a charge transfer process that requires direct contact of the molecules with the metal surface [21]. Thus, it would be crucial to develop approaches able to control these factors.

By keeping these aspects in mind, we have developed an SERS-based method for ultrasensitive detection of a biomolecular marker by exercising care in controlling and optimizing the geometry of the SERS probe with respect to the metal surface, also in connection with the possibility of having a contribution from a charge transfer mechanism. In this respect, we exploited a molecule derived from fluorescein called Samsa and containing an activable thiol group able to form a covalent bond with the gold nanoparticles (NPs). Indeed, we recently showed that Samsa bound to gold NPs undergoes an electron transfer process under light illumination as well as a drastic quenching of its intrinsic high fluorescence signal at the level of a single molecule [22]. Accordingly, here Samsa was stably bound to gold NPs by exploiting the thiol group, reaching a controlled short distance between the molecule and the metal surface, to achieve a significantly enhanced Raman signal.

As a biological marker, we chose thrombin, a serine protease whose concentration level in blood has high relevance in some pathologies [23,24]. Whereas thrombin is nearly absent in blood in normal conditions, its presence—even at a very low concentration—could be indicative of coagulation abnormalities [25]. Moreover, because a variety of sensors for thrombin, using different techniques and approaches and covering a wide concentration

* Corresponding author.
E-mail address: bizzarri@unitus.it (A.R. Bizzarri).

[1] *Abbreviations used:* SERS, surface-enhanced Raman spectroscopy; EM, electromagnetic; NP, nanoparticle; AFM, atomic force microscopy; APTMS, (3-aminopropyl)triethoxy-silane; PBS, phosphate-buffered saline; CCD, charge-coupled device; NA, numerical aperture; NC, noncontact; S/N ratio, signal-to-noise ratio.

0003-2697/$ - see front matter © 2009 Elsevier Inc. All rights reserved.
doi:10.1016/j.ab.2009.06.034

range, have been developed [26–31], including our previous work [32], this protein may represent a suitable benchmark to test the capabilities of a new approach for ultrasensitive detection.

The capability of thrombin to form a complex with antithrombin, through a biorecognition process, was exploited to promote the capture of thrombin–Samsa-labeled NPs from a substrate previously functionalized with antithrombin biomolecules. Heparin was added to the substrate to stably anchor the NPs to the substrate [33]. Indeed, heparin, an anionic polysaccharide with high affinity for antithrombin, is able to induce the formation of an irreversible complex between thrombin and antithrombin. The capture of the functionalized gold NPs from the substrate was investigated by atomic force microscopy (AFM) imaging; with the percentage of gold NPs stably deposited on the substrate also being estimated.

The applied strategy, based on the enhanced SERS signal of Samsa and the biorecognition-assisted capture, allowed us to detect thrombin at a concentration in the picomolar (pM) range. Such a detection level is comparable to that we obtained recently by the same biorecognition system but a different SERS probe [32]. Indeed, in the previous work, we used a bifunctional molecule having, on one end, a tail able to bind to a gold NP and, on the other end, a diazonium moiety capable of targeting aromatic lateral chains of protein. However, the method presented here can be more easily extended to the detection of other kinds of biomolecules and does not require preliminary treatment of the Raman probe to promote a reaction with protein molecules. In this respect, it represents a good starting point for the development of ultrasensitive biosensors in early biodiagnostics. Furthermore, the combined approach, exploiting SERS and AFM imaging, might deserve some interest from the perspective of implementing innovative multisensing detection.

Materials and methods

Gold NP colloidal solution ($HAuClO_4?3H_2O$), 50 nm diameter (distribution ~ 20%), with 4.5×10^{10} particles/ml (corresponding to a concentration of 75 pM) were purchased from Ted Pella. Thrombin (34 kDa), antithrombin III (58 kDa) from human plasma, heparin sodium salt, and all other chemicals were purchased from Sigma–Aldrich.

Samsa (10 mg, A-685, Molecular Probes) was dissolved in 1 ml of 0.1 M sodium hydroxide and incubated for 15 min to remove the acetyl group protecting the thiol. The solution was then neutralized with 6 M chloridric acid and buffered with sodium phosphate at pH 7.0. The activated Samsa was then incubated with a suspension of gold NPs to promote the attachment to gold via the thiol group [34]. The formation of the S–Au bond between Samsa and gold NPs was witnessed by the disappearance of the band centered at 2550 cm^{-1} inherent in the stretching vibration of S–H when Samsa is bound to gold NPs (see the inset of Fig. 1C) [35]. Then Samsa-labeled NPs were incubated for approximately 2 h with a thrombin solution. The concentration of thrombin in the final samples was in the range of 1 pM to 10 nM, corresponding to approximately 1 to 10^4 ng/cm^2. At the lowest concentration of thrombin, a 1:1 ratio between biomolecules and gold NPs was reached. The resulting sample was then deposited on the capture substrate.

Glass substrates, previously cleaned with piranha solution (30% H_2O_2/70% H_2SO_4), were immersed in 7% (3-amino-propyl)triethoxy-silane (APTMS) to form a self-assembled monolayer [36]. Subsequently, glasses were reacted with 1% glutaraldehyde solution for 1 h at room temperature and washed thoroughly with Milli-Q water. These glutaraldehyde-treated glasses were then reacted with 60 µl of antithrombin III (10^{-6} M) in phosphate-buffered saline (PBS, 46 mM, pH 7.0) for 24 h at 0 °C. Afterward, 30 µl of heparin sodium salt (3.2 mM) in PBS (46 mM, pH 7.5) was added.

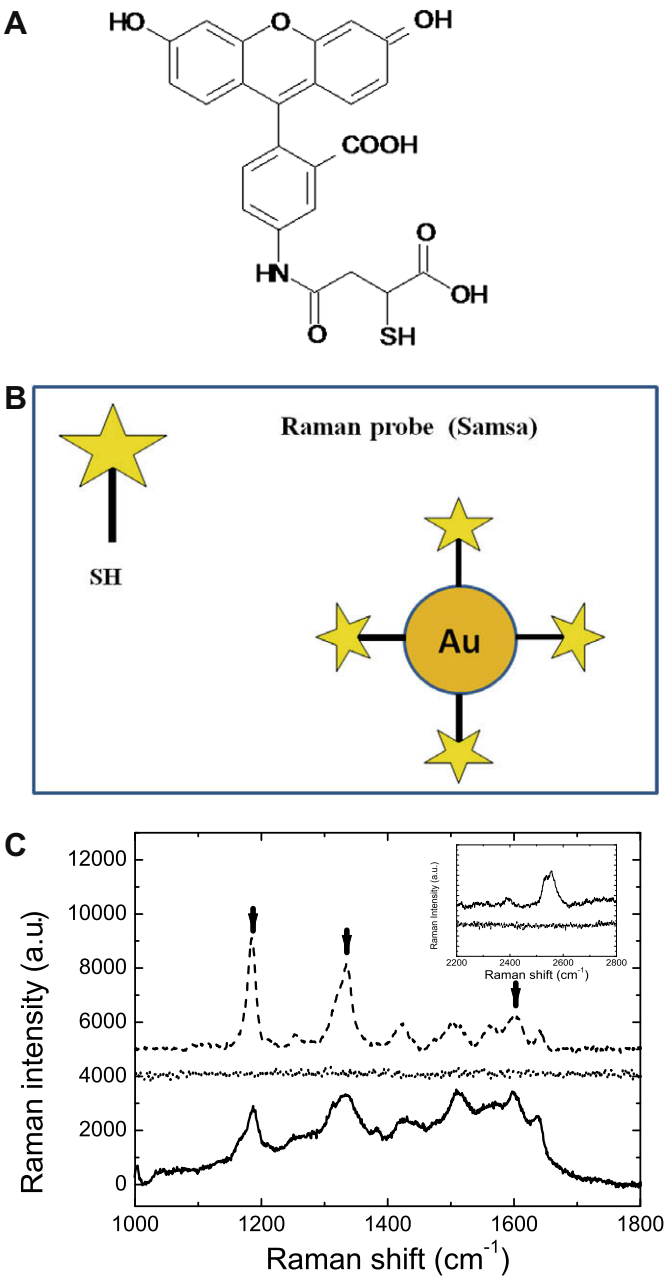

Fig. 1. (A) Chemical structure of Samsa. (B) Sketch of the labeling of gold NPs with Samsa. (C) Raman spectrum of Samsa at 10 mM (dashed line) and SERS spectrum of gold NPs labeled with Samsa at a concentration of 30 nm (continuous line). Both of the spectra were obtained from a dried drop of solution deposited on a glass with an integration time of 60 s. The arrows mark the frequencies at 1184, 1330, and 1585 cm^{-1}. a.u., arbitrary units.

The functionalized glasses were incubated overnight with 70 µl of gold NPs marked with thrombin and Samsa at 4 °C. Then the glasses were washed several times with Milli-Q water to remove excess NPs. As a control system, functionalized glasses were incubated with 70 µl of NPs marked only with Samsa and then rinsed.

SERS spectra were recorded by a Labram confocal setup (Jobin–Yvon) equipped with a charge-coupled device (CCD) Peltier-cooled detector and a single-grating spectrograph with an 1800-g/mm grating allowing a resolution of 5 cm^{-1}. The microscope objective was 100× with a numerical aperture (NA) of 0.9 producing a laser

spot size of approximately 1 μm in diameter. The source was a He–Ne ion laser (Melles Griot) providing 632.8 nm radiation with the power kept below 5 mW.

AFM measurements in noncontact (NC) mode were performed by XE-100 AFM (PSIA) equipped with a 50-μm scanner. Standard silicon cantilevers (RTESP, Veeco Probes), with a typical spring constant of 20 to 80 N/m and a nominal radius of curvature between 10 and 20 nm, were used. The typical scan rate was 2 Hz.

Results and discussion

The SERS method developed for detecting biological markers at very low concentrations exploits as a Raman probe a derivative of fluorescein, called Samsa, containing an activable thiol group (Fig. 1A). This thiol was used to covalently bind Samsa to gold NPs (Fig. 1B) to obtain a controlled short distance between the Samsa molecule and the metal surface for an optimized SERS signal. Indeed, a short distance between the molecule and the metal surface can give rise to high EM enhancement, whereas the presence of a covalent bond favors a charge transfer mechanism, resulting in an additional chemical enhancement [15].

The vibrational features of Samsa, free and bound to gold NPs, were analyzed by Raman spectroscopy with an exciting wavelength of 632 nm in the 900 to 1800-cm^{-1} region. The spectrum from a dried drop of 10 mM solution of Samsa at pH 7.0 exhibits several lines (Fig. 1C, dashed curve) that correspond to the vibrational modes of the π-electron system of oxygen and xanthene moiety of Samsa, in complete agreement with those observed for fluorescein [37]. We chose, as vibrational fingerprints of the Samsa Raman probe to be followed, the peaks at 1184, 1330, and 1585 cm^{-1} (see arrows in Fig. 1C), which have been attributed to the C–OH and C–C stretching modes [37,38].

The SERS spectrum from a dried drop of a solution obtained on reacting 30 nM Samsa with 50-nm-diameter gold NPs is shown in Fig. 1C (continuous curve). At these concentrations, approximately 400 Samsa molecules, corresponding to a surface coverage of approximately 50% , were estimated to be bound to each NP [39]. The SERS spectrum of Samsa shows several lines whose positions well match those observed in the Raman spectrum of Samsa alone (Fig. 1C, dashed line). This means that the vibrational features of Samsa are substantially preserved on its anchoring to gold NPs via the thiol group. On the other hand, the Raman spectrum of Samsa at the concentration of 30 nM, with the same integration time, does not reveal any signal over the noise (see dotted curve in Fig. 1C). Accordingly, high enhancement of the Raman cross section of Samsa molecules conjugated to gold NPs occurs. At the same time, the overall contribution of free Samsa molecules to the SERS spectrum is considered as negligible.

The slight changes in the relative line intensity between the SERS and the Raman spectra find a correspondence with what is commonly observed in the SERS spectra of several molecular systems. Indeed, in proximity of a metal surface, some changes in the structural and dynamical behavior of the molecules might occur (see, e.g., Refs. [20,40,41]). On the other hand, the presence of the large background underlying the SERS spectrum could yield a slight shift of the Raman lines [17]. Therefore, the substantial preservation of the Raman vibrational features registered in connection with good stability in time suggests that Samsa bound to gold NPs is a suitable Raman probe to be exploited in optical biosensing.

The Samsa-labeled gold NPs, sketched in Fig. 1B, were then conjugated with the biological marker. In this respect, we chose thrombin, a serine protease that converts soluble fibrinogen into insoluble strands of fibrin and whose presence is involved in blood diseases [42,43]. The conjugation of Samsa-labeled gold NPs with thrombin was achieved by exploiting electrostatic interactions between thrombin, which possesses (at pH 7.0) an excess of groups with positive charges, and gold NPs, which are negatively charged [44,45]. The SERS spectra of Samsa-labeled NPs incubated with thrombin in the concentration range of 1 pM to 10 nM do not show any substantial difference from those of NPs labeled only with Samsa (not shown). This could be reasonably due to a rather low Raman cross section of thrombin in comparison with that of Samsa.

The effective adsorption of thrombin to gold NPs was monitored by optical spectroscopy. The optical spectrum of Samsa conjugated with gold NPs is shown in Fig. 2 (dashed line). The spectrum is dominated by a band at approximately 530 nm that can be ascribed to the localized surface plasmons due to collective oscillations of conductive electrons in gold NPs [46]. The addition of thrombin to Samsa-labeled gold NPs yields a red shift of the surface plasmon band together with an increase of the intensity (continuous line in Fig. 2). Such a shift can be explained in terms of a modulation of the plasmon resonance through a change of the refractive index of the medium surrounding the NPs, as induced by the adsorption of thrombin [47], supporting the adsorption of thrombin on gold NPs.

In our approach, we were interested in putting into relationship the detection of the SERS signal of the Raman probe Samsa with the presence of thrombin. With such an aim, we prepared a substrate containing a receptor able to capture the biological marker through a biorecognition process. More specifically, the capture substrate consists of a glass coated with silane and glutaraldehyde and reacted with the receptor (antithrombin and heparin), which is known to form an irreversible complex with thrombin [48]. To promote such a biorecognition process, a drop of the solution from thrombin–Samsa-labeled gold NPs (Fig. 3A) was deposited on the capture substrate. The system was washed several times with Milli-Q water successively. In such a way, the functionalized NPs that had not reacted with the capture substrate were washed out, whereas the remaining ones were expected to be trapped through the formation of a strong complex between thrombin and antithrombin (Fig. 3B). Accordingly, a deposition of the NPs on the top of the capture substrate was expected to occur. This would result in a change in the topological features of the substrate with the appearance of new spots, which can be detected by NC–AFM imaging [49]. With this aim, we previously characterized the substrates by AFM after immobilization of antithrombin and heparin. The substrates functionalized with

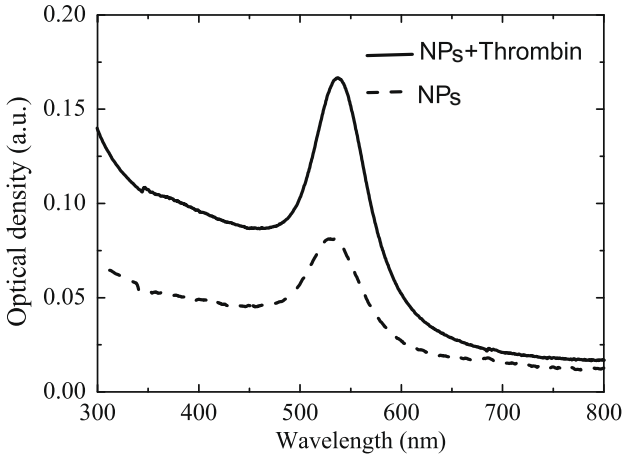

Fig. 2. Optical density spectrum of 50-nm-diameter gold NPs at pH 7.0 (dashed line) and of gold NPs incubated with thrombin at a concentration of 30 nM (continuous line).

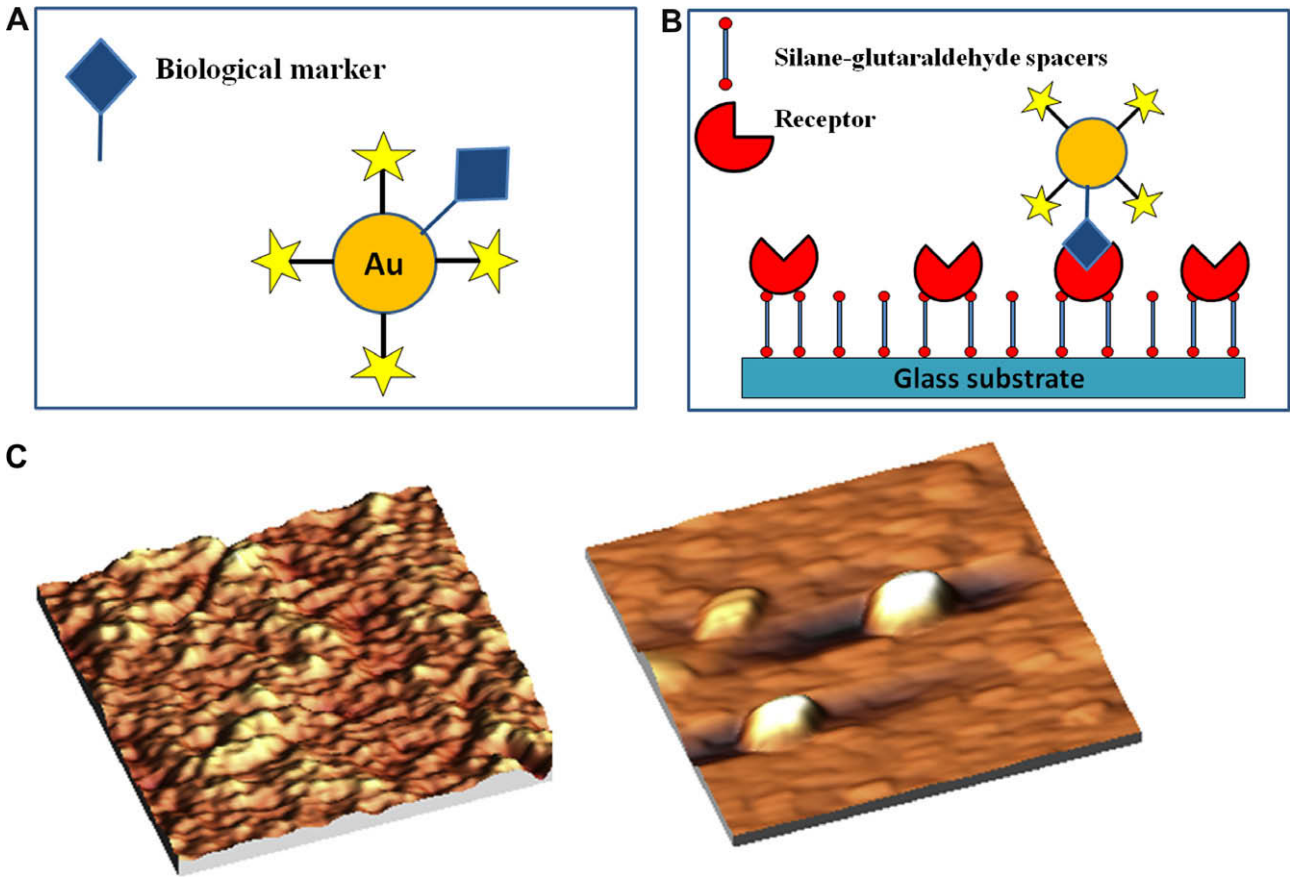

Fig. 3. (A) Sketch of the adsorption of thrombin to Samsa-labeled gold NPs. (B) Schematic representation of the procedure followed for promoting a biorecognition process between the marker adsorbed on gold NPs and the receptor immobilized on the substrate. (C) NC–AFM three-dimensional images (1×1 μm) of the functionalized substrate coated with antithrombin and heparin before (left: z range = 2 nm) and after (right: z range = 45 nm) deposition of gold NPs.

silane and glutaraldehyde exhibited a rough structure with a roughness parameter R_q of 1.2 ± 0.2 nm. On incubating these functionalized substrates with antithrombin and heparin, the roughness parameter R_q decreased to 0.5 ± 0.2 nm. After adding a drop of solution containing Samsa-labeled gold NPs also marked with thrombin at a picomolar concentration, we observed the appearance of large, rather regular spots in the AFM images. Fig. 3C shows representative three-dimensional AFM images of the capture substrate before (left) and after (right) deposition of functionalized gold NPs. The histogram of the cross-section analysis of 50 newly appearing large spots shows a single mode distribution with an average of 44 nm and a standard deviation of 6 nm (see Fig. 4). These values are consistent with the nominal values of gold NPs of 50 nm with scattering of approximately 20%. On the other hand, the lateral dimension of the spots (see, e.g., Fig. 4A) appears to be much larger due to the convolution of the image with the tip shape [50]. An estimation of the true lateral size of the imaged NPs can be obtained by taking into account that, for a spherical object imaged by a tip of radius of curvature R, the real diameter d is given by the relation $d = W^2/8R$, where W is the measured apparent width [51]. For the marked spot shown in Fig. 4A, the measured width of approximately 100 nm corresponds to an effective lateral size of approximately 60 nm, in satisfactory agreement with the expected dimension of 50 nm.

For a control, we repeated the experiment by depositing a drop of solution containing Samsa-labeled NPs without thrombin. After extensive washing, no regular large spots corresponding to gold NPs were detected, in agreement with the fact that no biorecognition process takes place due to the absence of thrombin.

The investigation of the morphological properties of the substrates by AFM was also exploited to estimate the percentage of NPs effectively deposited on the substrate. A statistical analysis performed by collecting five sets of 20 1×1-μm images evidenced the presence of 41 ± 4 spots. Notably, the images were acquired by progressively moving the substrate along the same direction to be sure to sample different areas of the substrate. By taking into account the concentration of the functionalized NPs in solution (4.9×10 NPs/ml), a drop of 70 μl of colloidal solution contains approximately 3.4×10^8 NPs. Under the assumption that a drop of NP solution is deposited on a surface of approximately 60 mm^2, approximately 120 NPs are expected to be found on the surface of 20 μm^2. This corresponds to a stable deposition of approximately 30% of the available NPs on the substrate. Such an estimation suggests that only a relatively small fraction of functionalized NPs gives rise to a successful interaction with the substrate. This could be due to a concomitant action of different factors. For example, the scattered orientations of antithrombin molecules, anchored to the substrate through exposed lysine residues, might reduce the interaction capability with thrombin, which in turn might also assume different orientations.

The sample, obtained on depositing thrombin–Samsa-labeled NPs, was finally scanned under the microscope objective of the Raman equipment to reveal the vibrational fingerprints of Samsa. By taking into account the AFM analysis, approximately 2 NPs should be found, on average, in a spot of 3 μm^2. A representative SERS

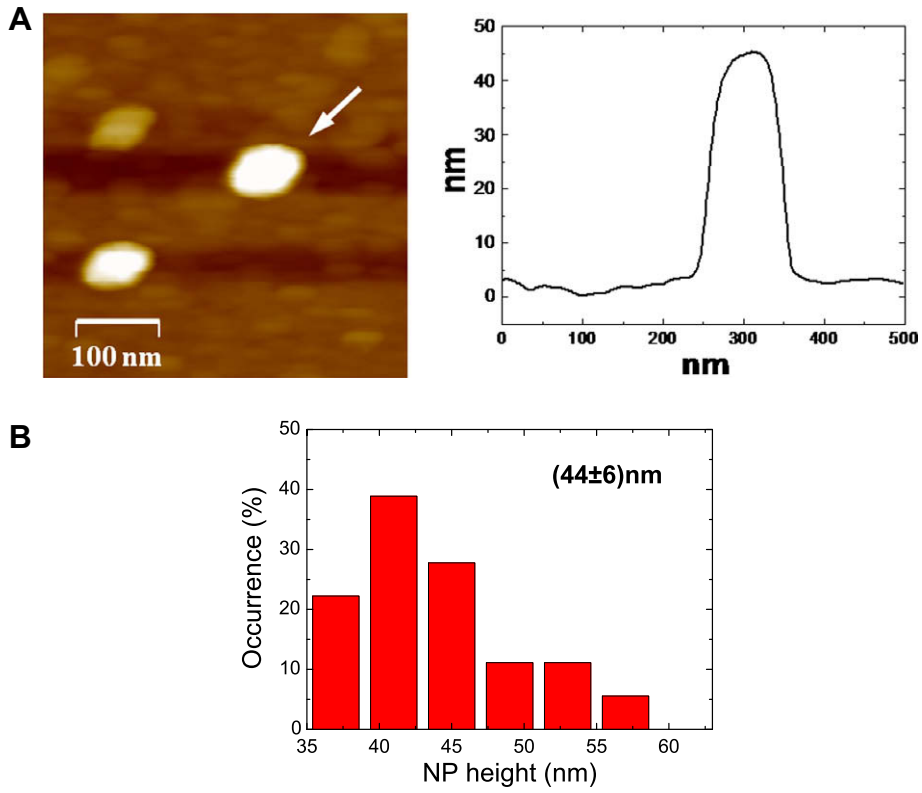

Fig. 4. (A) NC–AFM image of functionalized substrate coated with antithrombin and heparin and after deposition of gold NPs and the cross section analysis of the large spot indicated by the arrow. (B) Histogram and related averages and standard deviations of the height for a set of 50 large regular spots.

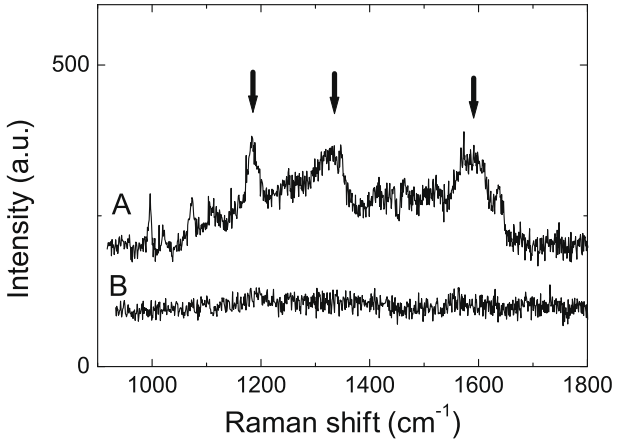

Fig. 5. (A) SERS spectrum of the capture substrate on depositing thrombin–Samsa-labeled NPs (with thrombin at 1 pM). (B) SERS spectrum of the capture substrate on depositing Samsa-labeled NPs without thrombin. Both of the spectra were recorded with an integration time of 60 s. The arrows mark the frequencies at 1184, 1330, and 1585 cm^{-1}. a.u., arbitrary units.

spectrum from an active site, as obtained from a sample containing thrombin at a concentration of 1 pM, is shown in Fig. 5 (curve A). Similar spectra were detected in other sites of the sample, with slight changes in the line position and in the relative intensities of the lines being observed from spectrum to spectrum. The vibrational fingerprints of Samsa are clearly visible (see the arrows in Fig. 5), and due to the formation of the biorecognition-based complex between thrombin and antithrombin, they signal the presence of the biological marker to be detected. Such a detection value is comparable to that obtained for the most sensitive biosensor currently developed for thrombin [27]. However, because only 30% of functionalized NPs are actually deposited on the capture substrate, the detection level of thrombin could be increased by improving the efficiency of the NP deposition.

The signal-to-noise (S/N) ratio in the SERS spectrum of curve A in Fig. 5 appears to be lower than that observed in Samsa-labeled gold NPs on glass (see Fig. 1C). More specifically, the S/N ratio passes from 10 for Samsa-labeled gold NPs deposited on glass to approximately 3 for the final capture substrate. This is consistent with the observation that only approximately 30% of Samsa-labeled gold NPs remain trapped on the capture substrate.

Notably, the Raman spectra from the antithrombin-coated substrate after depositing a drop of solution containing Samsa-labeled gold NPs without thrombin do not reveal any signal from Samsa (see Fig. 5, curve B), in agreement with the evidence that no large spots appear in the AFM images. We should note in passing that the capture substrate, in which antithrombin and heparin were deposited, does not show any appreciable Raman signal.

It should be remarked that, while at a concentration of thrombin below a threshold of 1 pM, the Raman signal of Samsa is distinguishable with difficulty over the noise, AFM imaging is able to reveal the presence of gold NPs on the substrate, indicative of the presence of the marker on the substrate. The high sensitivity shown by AFM suggests that such a technique can be combined with SERS for ultrasensitive detection of biomolecules opening new scenarios in multisensing.

Conclusions

Samsa molecules covalently bound to gold NPs exhibit high enhancement of Raman signal with vibrational features well distinguishable and stable in time. Accordingly, it appears to be a suitable Raman probe to be used in signaling the occurrence of a biorecognition process between marker and receptor. Using thrombin as

biological marker adsorbed on Samsa-labeled gold NPs and using antithrombin as receptor deposited on the capture substrate, we were also able to reveal the biological marker at a concentration down to 1 pM. Such an approach can easily be extended to other biomolecules provided that a strong alternative attachment for their binding to gold NPs is reached. The combined use of AFM imaging, which allowed us to verify the formation of the complexes on the substrate and to estimate the number of gold NPs trapped on the substrate, surprisingly resulted in detecting the presence of the biological marker even at a lower concentration. In this respect, the integration of SERS with AFM opens a new perspective for multisensing applications in bionanomedicine to perform high-throughput screening of biomolecules with very high sensitivity.

Acknowledgment

Thanks are due to Fabio Domenici for providing optical spectra on thrombin–gold nanoparticles.

References

[1] A.P. Turner, Biosensors: sense and sensitivity, Science 290 (2000) 1315–1317.
[2] C.A. Rowe, S.B. Scruggs, M.J. Feldstein, J.P. Golden, F.S. Ligler, An array immunosensor for simultaneous detection of clinical analytes, Anal. Chem. 71 (1999) 433–439.
[3] N.L. Rosi, C.A. Mirkin, Nanostructures in biodiagnostics, Chem. Rev. 105 (2005) 1547–1562.
[4] N.V. Lavrik, M.J. Sepaniak, P.G. Datskos, Cantilever transducers as a platform for chemical and biological sensors, Rev. Sci. Instrum. 75 (2004) 2229–2253.
[5] T. Hianik, V. Ostatná, Z. Zajacová, E. Stoikova, G. Evtugyn, Detection of aptamer–protein interactions using QCM and electrochemical indicator methods, Bioorg. Med. Chem. Lett. 15 (2005) 291–295.
[6] K. Kneipp, Y. Wang, H. Kneipp, L.T. Perelman, I. Itzkan, R.R. Dasari, M.S. Feld, Single molecule detection using surface-enhanced Raman scattering, Phys. Rev. Lett. 70 (1996) 1667–1670.
[7] S. Nie, S.R. Emory, Probing single molecules and single nanoparticles by surface-enhanced Raman scattering, Science 275 (1997) 1102–1106.
[8] H. Xu, E.J. Bjerneld, M. Käll, L. Börjesson, Spectroscopy of single hemoglobin molecules by surface enhanced Raman scattering, Phys. Rev. Lett. 86 (1999) 4357–4360.
[9] A.R. Bizzarri, S. Cannistraro, Surface-enhanced resonance Raman spectroscopy signals from single myoglobin molecules, Appl. Spectrosc. 56 (2002) 1531–1537.
[10] Y.C. Cao, R. Jin, J.M. Nam, C.S. Thaxton, C.A. Mirkin, Raman dye-labeled nanoparticle probes for proteins, J. Am. Chem. Soc. 125 (2003) 14676–14677.
[11] X. Su, J. Zhang, L. Sun, T.W. Koo, S. Chan, N. Sundararajan, M. Yamakawa, A.A. Berlin, Composite organic–inorganic nanoparticles (COINs) with chemically encoded optical signatures, Nanoletters 5 (2005) 49–54.
[12] M. Culha, D. Stokes, L.R. Allain, T. Vo-Dinh, Surface-enhanced Raman scattering substrate based on a self-assembled monolayer for use in gene diagnostics, Anal. Chem. 75 (2003) 6196–6201.
[13] S.G. Peen, M.J. Natan, Nanoparticles for bioanalysis, Curr. Opin. Chem. Biol. 7 (2003) 609–615.
[14] M.D. Porter, R.J. Lipert, L.M. Siperko, G. Wang, R. Narayanan, SERS as a bioassay platform: fundamentals, design, and applications, Chem. Soc. Rev. 37 (2008) 1001–1011.
[15] A. Campion, P. Kambhampati, Surface enhanced Raman scattering, Chem. Soc. Rev. 127 (1998) 241–250.
[16] M. Moskovits, Surface-enhanced spectroscopy, Rev. Mod. Phys. 57 (1985) 783–826.
[17] A. Otto, I. Mrozek, H. Grabhorn, W. Akemann, Surface-enhanced Raman scattering, J. Phys. Condens. Matter. 4 (1992) 1143–1212.
[18] A.R. Bizzarri, S. Cannistraro, Evidence of electron-transfer in the SERS spectra of a single iron–protoporphyrin IX molecule, Chem. Phys. Lett. 395 (2004) 222–226.
[19] Y. Fang, N.H. Seong, D.D. Dlott, Measurement of the distribution of site enhancements in surface-enhanced Raman scattering, Science 311 (2008) 388–391.
[20] A.M. Michaels, M. Nirmal, L.E.M. Brus, Surface enhanced Raman spectroscopy of individual rhodamine 6G molecules on large Ag nanocrystals, J. Am. Chem. Soc. 121 (1999) 9932–9939.
[21] A.R. Bizzarri, S. Cannistraro, SERS and tunneling spectroscopy investigation of iron–protoporphyrin IX adsorbed on a silver tip, J. Phys. Chem. B 10 (2005) 16571–16574.
[22] F. Cannone, G. Chirico, A.R. Bizzarri, S. Cannistraro, Quenching and blinking of fluorescence of a single dye molecule bound to gold nanoparticles, J. Phys. Chem. B 110 (2006) 16491–16498.
[23] M.T. Stubbs, W. Bode, The clot thickens: clues provided by thrombin structure, Trends Biochem. Sci. 20 (1995) 23–28.
[24] J.A. Huntington, T.P. Baglin, Targeting thrombin-rational drug design from natural mechanisms, Trends Pharmacol. Sci. 24 (2003) 589–595.
[25] E. Di Cera, Thrombin as procoagulant and anticoagulant, J. Thrombosis Haemostasis 5 (2007) 196–202.
[26] S. Centi, S. Tombelli, M. Minurri, M. Mascini, Aptamer-based detection of plasma proteins by an electrochemical assay coupled to magnetic beads, Anal. Chem. 79 (2007) 1466–1473.
[27] Y. Xu, L. Yang, X. Ye, P. He, Y. Fang, An aptamer-based protein biosensor by detecting the amplified impedance signal, Electroanalysis 18 (2006) 1449–1456.
[28] D.R. Bing, R.J. Feldmann, J.W. Fenton II, Structure–function relationships of thrombin based on the computer-generated three-dimensional model of the B chain of bovine, Error! Hyperlink reference not valid, Ann. NY Acad. Sci. 485 (1986) 5–15.
[29] H.M. So, K. Won, Y.K. Kim, B.K. Kim, B.H. Ryu, P.S. Na, H. Kim, J.O. Lee, Single-walled carbon nanotube biosensors using aptamers as molecular recognition elements, J. Am. Chem. Soc. 127 (2005) 11906–11907.
[30] B. Basnar, R. Elnathan, I. Willner, Following aptamer–thrombin binding by force measurements, Anal. Chem. 78 (2006) 3638–3642.
[31] V. Pavlov, Y. Xiao, B. Shlyahovsky, I. Willner, Aptamer-functionalized Au nanoparticles for the amplified optical detection of thrombin, J. Am. Chem. Soc. 126 (2004) 11768–11769.
[32] A.R. Bizzarri, S. Cannistraro, SERS detection of thrombin by protein recognition using functionalized gold nanoparticles, Nanomed. Nanotechnol. Biol. Med. 3 (2007) 306–310.
[33] U. Lindahl, G. Backstrom, L. Thunberg, The antithrombin-binding sequence in heparin, J. Biol. Chem. 258 (1983) 9826–9830.
[34] A. Ulman, Formation and structure of self-assembled monolayers, Chem. Rev. 96 (1996) 1533–1554.
[35] M. Osawa, N. Matsuda, K. Yoshii, I. Uchida, Charge transfer resonance Raman process in surface-enhanced Raman scattering from *p*-aminothiophenol adsorbed on silver: Herzberg–Teller contribution, J. Phys. Chem. 98 (1994) 12702–12707.
[36] R.G. Freeman, K.C. Grabar, K.J. Allison, R.M. Bright, J.A. Davis, A.P. Guthrie, M.B. Hommer, M.A. Jackson, P.C. Smith, D.G. Walter, M.J. Natan, Self-assembled metal colloid monolayers: an approach to SERS substrates, Science 267 (1995) 1629–1632.
[37] L. Wang, A. Roitberg, C. Meuse, A.K. Gaigalas, Raman and FTIR spectroscopies of fluorescein in solutions, Spectrochim. Acta A 57 (2001) 1781–1791.
[38] P. Hildebrandt, M. Stockburger, Surface enhanced resonance Raman study on fluorescein dyes, J. Raman Spectrosc. 17 (1986) 55–58.
[39] L.F. Pease III, D. Tsai, R.A. Zangmeister, M.R. Zachariah, M.J. Tarlov, Quantifying the surface coverage of conjugate molecules on functionalized nanoparticles, J. Phys. Chem. C 111 (2007) 17155–17157.
[40] A. Weiss, G. Haran, Time-dependent single-molecule Raman scattering as a probe of surface dynamics, J. Phys. Chem. B 105 (2001) 12348–12354.
[41] A.R. Bizzarri, S. Cannistraro, Temporal fluctuations in the SERRS spectra of single iron–protoporphyrin IX molecule, Chem. Phys. 290 (2003) 297–306.
[42] C.A. Holland, A.T. Henry, H.C. Whinna, F.C. Church, Effect of oligodeoxynucleotide thrombin aptamer on thrombin inhibition by heparin cofactor II and antithrombin, FEBS Lett. 484 (2000) 87–91.
[43] M.T. Stubbs, W. Bode, A player of many parts: the spotlight falls on thrombin structure, Thromb. Res. 69 (1993) 1–58.
[44] H. Zhao, B. Yuan, X. Dou, The effects of electrostatic interaction between biological molecules and nano-metal colloid on near-infrared surface-enhanced Raman scattering, J. Optics A 6 (2004) 900–905.
[45] E. Katz, I. Willner, Integrated nanoparticle–biomolecule hybrid systems: synthesis, properties, and applications, Angew. Chem. Intl. Ed. 43 (2004) 6042–6108.
[46] S. Link, M.A. El-Sayed, Spectral properties and relaxation dynamics of surface plasmon electronic oscillations in gold and silver nanodots and nanorods, J. Phys. Chem. B 103 (1999) 8410–8426.
[47] J.N. Anker, W.P. Hall, O. Lyandres, N.C. Shah, J. Zhao, R.P. Van Duyne, Biosensing with plasmonic nanosensors, Nat. Mater. 7 (2008) 442–453.
[48] U. Lindhal, G. Backstrom, M. Hook, L. Thunberg, L.A. Fransson, A. Linker, Structure of the antithrombin-binding site in heparin, Proc. Natl. Acad. Sci. USA 76 (1979) 3198–3202.
[49] B. Bonanni, S. Cannistraro, Gold nanoparticles on modified glass surface as height calibration standard for atomic force microscopy operating in contact and tapping mode, J. Nanotechnol. Online (2005) doi:10.2240/azojono0105.
[50] P. Markiewicz, M.C. Goh, Simulation of atomic force microscope tip–sample/sample–tip reconstruction, J. Vac. Sci. Technol. B 13 (1995) 1115–1118.
[51] J. Vesenka, M. Guthold, C.L. Tang, D. Keller, E. Delain, C. Bustamante, Substrate preparation for reliable imaging of DNA molecules with the scanning force microscope, Ultramicroscopy 42 (1992) 1243–1249.